Identification of a new natural gastric lipase inhibitor from star anise

Jannet Kamoun, Renaud Rahier, Mohamed Sellami, Imed Koubaa, Pascal Mansuelle, Régine Lebrun, Alexandra Berlioz-Barbier, Michele Fiore, Karine Alvarez, Abdelkarim Abousalham, et al.

Preprint of DOI: 10.1039/c8fo02009d

Identification of a new natural gastric lipase inhibitor from star anise

Jannet Kamoun[1,2,3], Renaud Rahier[3,§], Mohamed Sellami[1], Imed Koubaa[4], Pascal Mansuelle[5], Régine Lebrun[5], Alexandra Berlioz-Barbier[3], Karine Alvarez[6], Abdelkarim Abousalham[3], Frédéric Carrière[2], and Ahmed Aloulou[1,§,*]

[1] University of Sfax, National School of Engineering of Sfax, Laboratory of Biochemistry and Enzymatic Engineering of Lipases, Sfax 3038, Tunisia.

[2] Aix-Marseille University, CNRS, Bioénergétique et Ingénierie des Protéines, UMR 7281, Marseille 13009, France.

[3] Univ. Lyon, Université Lyon 1, Institut de Chimie et de Biochimie Moléculaires et Supramoléculaires (ICBMS), UMR 5246 CNRS, Métabolisme, Enzymes et Mécanismes Moléculaires (MEM^2), Villeurbanne 69622, France.

[4] University of Sfax, Faculty of Science of Sfax, Laboratory of Chemistry of Natural Products, Sfax 3038, Tunisia.

[5] Aix-Marseille University, CNRS, Institut de Microbiologie de la Méditerranée, Plateforme Protéomique, Formation de Recherche 3479, Marseille 13009, France.

[6] Aix-Marseille University, CNRS, Architecture et Fonction des Macromolécules Biologiques, UMR 7257, Marseille 13009, France.

[§] Present Address: University of Illinois at Chicago, Department of Chemistry, Chicago, Illinois 60607, USA.

[*] Corresponding author. Email: aloulou@uic.edu

Abbreviations

DGL, dog gastric lipase; HPL, human pancreatic lipase; LipY, mycobacterial Rv3097c-encoded lipase; SA, star anise; DMSO, dimethyl sulfoxide; M5ME, myricitrin-5-methyl ether; FFA, Free fatty acid; TC4, tributyrin; NaTDC, sodium taurodeoxycholate; SAPRF, star anise polyphenolic-rich fraction; MALDI-TOF-MS; matrix-assisted laser desorption ionization-time of flight mass spectrometry; PMF, peptide mass fingerprinting; TLC, thin layer chromatography; UPLC-HRMS, ultra-performance liquid chromatography high resolution hybrid quadrupole-time of flight mass spectrometry.

Abstract

Bioactive compounds identification and isolation from natural complex samples, even though being a difficult task, is of great interest in the drug discovery field. We describe here an innovative strategy for the identification of a new gastric lipase inhibitor from star anise for the treatment of obesity. After plant screening assays for gastric lipase inhibition, star anise was selected and investigated by bioactivity guided fractionation. MALDI-TOF mass spectrometry and peptide mass fingerprinting allowed the detection of an inhibitor covalently bound to the catalytic serine of gastric lipase. Mass-directed screening approach using UPLC-HRMS and accurate mass determination searching identified the flavonoid myricitrin-5-methyl ether (M5ME) as a lipase inhibitor. The inhibitory activity was rationalized based on molecular docking, showing that M5ME is susceptible to a nucleophilic attack by gastric lipase. Overall, our data suggest that M5ME may be considered as a potential candidate for future application as a lipase inhibitor for the treatment of obesity.

Keywords

Gastric lipase, inhibition; star anise, guided fractionation; mass spectrometry, molecular docking.

1. Introduction

Gastric and pancreatic lipases play a key role in gastrointestinal digestion of dietary fat suggesting that they may represent a drug target for the treatment of obesity [1, 2]. Gastric lipase is the key enzyme for the gastrointestinal digestion of dietary triglycerides [3]. Lipid digestion is initiated in the stomach by the acid stable gastric lipase and continues in the duodenum through the synergistic actions of gastric lipase and colipase-dependent pancreatic lipase, leading to the formation of absorbable monoglycerides and free fatty acids (FFA) [4]. Inhibiting these lipases to reduce fat absorption is the main pharmacological approach adopted for the treatment of obesity [5]. Orlistat, a hydrogenated derivative of lipstatin derived from *Streptomyces toxitricini*, is the only FDA-approved anti-obesity drug that specifically targets digestive lipases [6]. This drug is an active site-directed inhibitor that reacts with the nucleophilic serine residue of the catalytic triad of digestive lipases within the gastrointestinal tract [7]. However, Orlistat, which is considered relatively too expensive to afford, is also known to inhibit various other enzymes and could lead to undesirable side effects, which might affect its current clinical use [8]. Therefore, looking for new cost-effective digestive lipase inhibitors is highly demanded nowadays.

Much interest has been shifted on plant polyphenols that have been reported to play a significant role in the prevention of overweight and obesity [9, 10]. More precisely, polyphenolic-rich extracts from plant sources have been reported to inhibit pancreatic lipase *in vitro* [11-14].

Bioactivity guided fractionation is a useful approach for the chemical and biological screening of complex plant extracts [15, 16]. Mass spectrometry (MS)-based affinity approaches have emerged as effective tools in small-molecule drug discovery. In these approaches the mass spectrometer can be exploited to rapidly screen drug candidates for specific interactions

with targets of interest [17]. Coupling bioaffinity selection to MS has been developed in the screening of natural product extracts [18] and synthetic combinatorial libraries [19]. Accordingly, direct and indirect bioaffinity screening approaches have been used. In the indirect screening approach, the complex protein-ligand is dissociated prior the MS analysis, allowing thus the identification of the target ligand. Whereas, in the direct screening approach, the MS analysis can be directly performed on the whole complex [20]. With the availability of MS technologies, direct bioaffinity screening approach could be a potential way to facilitate tentative identification of the relevant compound within simplified natural mixtures.

UPLC-HRMS is a modern powerful tool to identify known and unknown compounds in a complex mixture. The use of UPLC-HRMS in combination with a QTOF mass spectrometer for target and non-target screening purposes has gained popularity in recent years [21]. Indeed, UPLC provides fast and high-resolution separation, which increases LC-MS sensitivity and minimizes matrix interference arising from minimal simple preparation. Coupling of UPLC system with QTOF-MS provides thus deep analysis on sample composition [22]. Although increasing applications focus on analyzing molecules present in a variety of samples, there have been no reports regarding UPLC-HRMS application for identifying lipase inhibitors from natural product mixture.

To identify a natural gastric lipase inhibitor from plants, we proposed herein a new strategy based on bioactivity guided fractionation along with direct bioaffinity screening using MALDI-TOF-MS and peptide mass fingerprinting (PMF), non-target screening using UPLC-HRMS, and *in silico* molecular docking.

2. Materials and methods

2.1. Preparation of plant crude extracts for screening study

Dried plant species, purchased from local markets, were cleaned and finely powdered using a grinder. All powdered samples were separately extracted by maceration technique using hexane, ethyl acetate, ethanol and water (1:10 w/v ratio). The different extracts were evaporated to dryness *in vacuo* yielding dried extracts. All extracts were dissolved in dimethyl sulfoxide (DMSO) to obtain a final concentration of 100 mg/mL and were assayed for their anti-lipase potency.

2.2. Bioactivity guided fractionation

Star anise crude phenolic extract (SACPE) was prepared from star anise powder *via* maceration in ethanol:water (7:3 v/v) (1:10 w/v ratio) for 24 hours. The solid-liquid mixture was filtered with fritted glass number 3. Then, the filtrate was evaporated to dryness *in vacuo* yielding dried SACPE.

Star anise powder was extracted with hexane (1:10 w/v) for 48 h to remove lipoidal material [23]. After filtration, the filtrate was evaporated under vacuum to yield star anise hexanic extract. The residue was air-dried at room temperature overnight to get the dried defatted star anise (DFSA). Thus, star anise phenolic extract (SAPE) was prepared from DFSA *via* maceration in ethanol:water (7:3 v/v) (1:10 w/v ratio) for 24 h.

SAPE was successively fractionated using liquid-liquid partition and solid-liquid extraction to obtain star anise polyphenol-rich fractions (SAPRF). In a first step, liquid-liquid partitioning of SAPE with ethyl acetate gives two fractions SAPRF1 and SAPRF2. These fractions were evaporated under vacuum (45 °C), lyophilized and subjected to the inhibition test against DGL activity. SAPE, SAPRF1 and SAPRF2 were then analyzed by TLC on aluminum sheets coated with 0.2 mm silica gel 60 to characterize their chemical profile. The migration was performed with a mixture of chloroform:methanol (8:2 v/v). After that, the

spots were revealed with iodine vapor. In a second step, SAPRF2 was re-suspended in ethyl acetate for solid-liquid extraction. After 3 hours of maceration, the mixture was filtered. Similarly, this second step led to two fractions, SAPRF3 and SAPRF4, that were dried under vacuum. Subsequently, SAPRF2 and the fraction produced (SAPRF3 and SAPRF4) were subjected to DGL inhibition test and TLC analysis under the same experimental conditions of the first step. SAPRF4 was thereby selected for further investigations. A flow chart for the preparation of various fractions from star anise powder is given in **Fig. 1**.

2.3. Lipase activity measurements using the pH-stat technique

Recombinant DGL [24], HPL [25], and LipY [26] were produced and purified as described previously. Pancreatic colipase was purified from lipid-free porcine pancreatic powder [27]. Lipases were stored in 150 mM NaCl buffered solutions (pH 6 for DGL, pH 7 for HPL, and pH 8 for LipY).

Enzymatic activity was assayed at 37 °C by measuring the amount of FFA released from a mechanically stirred tributyrin (TC4) emulsion, using 0.1 M NaOH with a pH-stat (Metrohm 718 STAT Titrino, Switzerland) adjusted to a fixed end point [28]. TC4 emulsions were formed by mixing 0.5 mL TC4 with 14.5 mL buffer solution. The activities of DGL were determined using the following assay solution: 150 mM NaCl, 2 mM sodium taurodeoxycholate (NaTDC), and 2 mM bovine serum albumin at pH 5.5 [24]. In the case of HPL, the activities were determined using the standard assay solution for PL: 0.3 mM Tris-HCl (pH 8.0), 150 mM NaCl, 2 mM $CaCl_2$, and 4 mM NaTDC, in the presence of 5 molar excess of colipase [25]. With LipY, the assay solution was 2.5 mM Tris-HCl (pH 7.5), 300 mM NaCl and 3 mM NaTDC [26]. Under the above assay conditions, enzymatic activities were expressed as international units: 1 U = 1 μmol FFA released per minute. The specific activities of DGL, HPL, and LipY, expressed in U per mg of pure enzyme, were found to be 340 ± 21, 8021 ± 79 and 129 ± 2 U/mg, respectively.

2.4. Assay for anti-lipase activity

The lipase-inhibitor pre-incubation method was used to test, in aqueous medium and in the absence of substrate, the possible direct reactions between lipases and inhibitors [5]. Lipase-inhibitor pre-incubations were performed at 25 °C, at different times and at various inhibitor extract amounts (a_I), in presence of 4 mM NaTDC [5]. The final enzyme concentration in the incubation medium was 1 µM. The residual lipase activity was measured by the pH-stat. The amount of the inhibitor fraction (a_{I50}) and the half-inactivation time ($t_{½}$), corresponding to 50 % of residual enzyme activity, were determined.

In each case, control experiments were performed in the absence of inhibitor fraction but with the same volume of DMSO. It is worth noting that DMSO at a final volume concentration less than 10 % has no effect on the enzyme activity.

2.5. UPLC-HRMS experiment

The system used for UPLC-HRMS was an ultra-performance liquid chromatography Ultimate 3000 (Thermo Fisher Scientific, Villebon-sur-Yvette, France) coupled to a high-resolution hybrid quadrupole-time of flight mass spectrometer (Impact II, Bruker, Brême, Germany) equipped with electrospray ionization source (ESI) (Bruker, Brême Germany). Instrument control and data collection were performed using Data Analysis 5.0 software.

Chromatographic separation was performed on a polar C18 column (10 cm × 2.1 mm × 1.7 µm, Luna Omega, Phenomenex, France). The column oven temperature was set at 40 °C and an injection volume of 7 µL of the sample was loaded. The sample compounds were separated at a flow rate of 0.4 µL/min using (A) H_2O (Milli-Q) with 0.1 % formic acid and (B) acetonitrile with 0.1 % formic acid. The analytes were separated using the following gradient: from 0 % to 100 % of B in 30 min and kept constant for 5 min. The column was re-equilibrated for 10 min at the initial composition of the gradient before runs.

The ESI interface was operated on full scan mode (m/z 50-2000) in negative and positive ion mode. The parameters for the ESI ion source were as follows: the capillary voltage, 3.0 kV; the source temperature, 200 °C; the operating pressure of the nitrogen flow for the nebulizer gas, 45 Psi. Ultraviolet (UV) detectors measured the absorption over the range of 250 and 280 nm.

Before each acquisition batch, external calibration of high-resolution mass spectrometer was performed with a sodium formate cluster solution. The calibration solution was injected at the beginning of each run. MS/MS analyses were carried out with Data Dependent Acquisition mode for precursor ions with an intensity superior to 2000 counts using a stepping of collision energy ramp.

Annotation of each signal was performed by interrogation of different databases (ChemSpider, MassBank, Drugbank, HMDB) using a home-made software providing annotation of LC-MS data according to parent mass accuracy (< 5 ppm). After generation of a short list of potential candidates for each signal, the correlation of isotope patterns according to putative atomic compositions was checked to reduce the list of putative annotation (mSigma < 30). The investigation of experimental MS/MS data using web-based spectral database and/or *in silico* fragmentation tool as MetFrag© was necessary to obtain structural information and annotate more precisely each compound.

2.6. MALDI-TOF mass spectrometry analysis

DGL was pre-incubated for 30 min at 25 °C with a large excess of SAPRF4 (a_I = 30 µg) to abolish any residual lipolytic activity. A blank experiment was performed in the absence of SAPRF4. MALDI-TOF analysis of the entire non-inhibited or inhibited DGL was carried out with a Bruker Micoflex II mass spectrometer (Daltonik, Deutchland) using a saturated solution of α-cyano-4-hydroxycinnamic acid in acidified water (0.1 % TFA) and acetonitrile (30:70 v/v) [28]. Mass spectra were acquired in the positive ion mode, using the Flex Analysis™

192 software program (Bruker, Daltonik, Deutchland). Protein identification was performed using
193 the MASCOT™ version 2.2 search engine (Matrix Science, London, UK) and the NCBI
194 protein database. Theoretical and experimental peptide mass were obtained using the
195 BioTools™ software program (Bruker, Daltonik, Deutchland).

196 **2.7. Peptide mass fingerprinting**

197 Non-inhibited and inhibited DGL (with SAPRF4) were first separated by SDS-PAGE.
198 The protein bands were then excised from the gel and subjected to in-gel trypsin digestion
199 procedure as previously described [28]. For peptides identification, the in-gel digested peptides
200 were analyzed by a proteomic approach including MALDI-TOF/MS and electrospray
201 ionization (ESI) quadrupole time of flight (QTOF) MS/MS (Waters, Manchester) coupled
202 with a nano flow UPLC nano Acquity (Waters, Manchester). For UPLC-ESI-QTOF analysis,
203 the samples were dissolved in the loading buffer (3% acetonitrile/ 0.1 % TFA in water) and
204 desalted on a C18 nano trap (Symmerty C18, 180 µm × 2 cm, 5 µm, Waters) mounted on a 6-
205 port valve, before on line elution onto a C18 column (BEH 130 C18, 100 µm × 10 cm, 1.7
206 µm, Waters). Gradient elution was performed from 3 % to 50 % of mobile phase B (100 %
207 acetonitrile / 0.1 % formic acid) in A (0.1 % formic acid in water) for 30 min. The column
208 was rinsed for 6 min with 85 % of B and then brought back in 1 min to the initial condition.
209 Between each sample, a blank (injection of loading buffer only) was done using the same
210 chromatographic method. The peptides were detected into the mass spectrometer in a positive
211 ion mode using the MS^E mode. Data acquisitions of spectra were performed using the
212 Micromass software Protein Lynx Global Server 2.5.2 (Waters).

213 **2.8. Molecular docking**

214 *In silico* molecular docking of the M5ME inhibitor present in the active site of DGL
215 (PDB entry codes: 1K8Q - 2.70 Å resolution [24]) was performed using AutoDock Vina [29]
216 program under UCSF Chimera software [30]. The grid box size was chosen to fit the whole

active site cleft and to allow non-constructive binding positions. The inhibitor structure model was built using the Avogadro program [31]. Binding modes were scored and ranked based on the most favorable energies.

3. Results

3.1. Screening for anti-lipase properties of crude medicinal plant extracts

Twenty extracts, prepared from five medicinal plants with anti-obesity potential (*Illicium verum*, *Glycyrrhiza glabra*, *Salvia officinalis*, *Thymus vulgaris*, and *Rosmarinus officinalis*) [32], were screened for their inhibitory effect against DGL activity at an a_I value of 1 mg. The ethanolic extract of the fruits of *Illicium verum* (star anise) was found to have the strongest inhibitory activity (81 %) against DGL **(Table S1)**. While the ethanolic extract of *Rosmarinus officinalis* and the roots of *Glycyrrhiza glabra* showed a moderate inhibitory activity (43 and 44 %, respectively) toward DGL, the remaining medicinal plant extracts displayed weak inhibitory activities. Star anise was thereby selected for further processing.

3.2. Effect of defatting star anise on anti-lipase activity potency

Since star anise hexanic extract showed a weak inhibitory rate (18 %, **Table S1**) and a marked yield (around 7 %, data not shown), we evaluated the anti-lipase activity of phenolic extract from star anise before and after defatting sample. Thus, SACPE (non-defatted) and SAPE (defatted) extracts were prepared as described in the experimental section. Using an a_I value of 1 mg of each extract, the lipase inhibitory activity of SAPE (100 %) was higher than that of SACPE (89 %).

3.3. Bioactivity guided fractionation of SAPE

SAPE was fractionated using the scheme shown in **Fig. 1**. Two steps were used to fractionate SAPE. In the first step, the fractionation of SAPE led to SAPRF1 and SAPRF2, which were analyzed on TLC **(Fig. S1A)**. One can note that spots intensities in SAPRF1 and

SAPRF2 have increased compared to the initial extract (SAPE). DGL activity inhibitory test was conducted on each of these two fractions. At an a_I value of 500 µg of each fraction, SAPRF2 totally abolished DGL residual activity, while SAPRF1 led only to 25 % residual DGL activity. Subsequently, as SAPRF2 fraction was found to be more active, it was further subjected to a second fractionation step. Similarly, this latter led to SAPRF3 and SAPRF4 **(Fig. 1)** which were subjected to lipase activity inhibitory test and TLC analysis **(Fig. S1B)**. Unlike SAPRF3, SAPRF4 was found to display promising anti-lipase potency with 100 % DGL inhibition rate at an a_I value of 250 µg. Regarding TLC analysis, obtained results showed that SAPRF3 is moderately polar fraction, while SAPRF4 seems to have a strong polar character.

3.4. Evaluation of the inhibitory effect of SAPRF4 against lipases of medicinal interest

The inhibitory activity of the SAPRF4 fraction was evaluated against two mammalian digestive lipases (DGL and HPL) and one microbial lipase belonging to the hormone-sensitive lipase (HSL) family (LipY) [26]. With each lipase, linear kinetics corresponding to the FFAs (µmol) released *vs*. time (min) were obtained in the presence and absence of the inhibitor fraction. A dose-dependent effect was observed upon increasing the amount of SAPRF4 on DGL, HPL and LipY **(Fig. 2)**. At an a_I value of only 30 µg, DGL activity was totally abolished after a 30 min incubation period **(Fig. 2A)**, while HPL was strongly inactivated (96 %) at an a_I value of up to 1 mg **(Fig. 2B)**. However, LipY activity was not completely abolished even at a high SAPRF4 amount, showing a residual activity of ~20 % **(Fig. 2C)**. The a_{I50} values were found to be 7 µg, 82 µg and 5 µg for DGL, HPL and LipY, respectively **(Table 1)**, indicating that SAPRF4 is a potent inhibitor toward both DGL and LipY.

The influence of the incubation time on the level of inhibition of DGL, HPL and LipY by the SAPRF4 fraction was further investigated **(Fig. 2D-F)**. The residual activity of these

lipases decreased rapidly and reached a plateau value after approximately 30 min of incubation. From these inhibition curves, values of the half-inactivation times ($t_{½}$) were then determined and found to be 0.4 min, 0.6 min and 0.1 min for DGL, HPL and LipY, respectively **(Table 1)**. Such values reflect an extremely high rate of inhibition of these lipases by SAPRF4.

3.5. Analysis of the inhibitor-modified DGL complex with mass spectrometry

To investigate whether the inhibitory compound within SAPRF4 forms a covalent bond with the catalytic serine of DGL, MALDI-TOF-MS analysis was conducted on both non-inhibited and inhibited DGL. **Fig. 3** shows typical spectral recordings of untreated and treated DGL with SAPRF4. A clear shift in the molecular mass of DGL was observed reflecting a covalent binding of the inhibitor to the lipase.

To deduce the exact molecular mass of the inhibitor contained in the SAPRF4 fraction, PMF analysis of non-inhibited and inhibited DGL was performed. Results showed that the peptide L^{147}-K^{168} (LHYVGHSQGTTIGFIAFSTNPK) containing the catalytic S^{153} residue was detected at a molecular mass of 2376.05 Da with non-inhibited DGL **(Fig. 4A)**. This catalytic peptide appeared concomitantly with a second peptide detected at a molar mass of around 2414.82 Da. By contrast, when DGL was incubated with SAPRF4, a mass increase of + 489.52 Da was observed in the PMF spectrum for the catalytic peptide **(Fig. 4B)**, while the peptide detected at a molar mass of around 2414.82 Da remained unchanged. This mass shift (489.52 Da) observed here is supposed to correspond to the molecular mass of the natural inhibitor bound to DGL.

To tentatively identify the molecular formula and the structure of the phytochemical compound that binds covalently to DGL, we analyzed the SAPRF4 fraction by UPLC-HRMS. Seven major phenolic compounds have been identified **(Fig. S2A and Table S2)**. To empirically calculate their potential molecular formulas, various criteria have been used

among them: the isotopic pattern, the fragmentation pattern and the high-resolution accurate mass (with error below 0.4 ppm at the time of matching the theoretical mass with the measured mass). Mass-directed identification showed that the natural DGL inhibitor compound within the SAPRF4 fraction might correspond to myricitrin-5-methyl ether (M5ME) with a molecular mass of 479.1184 Da and a molecular formula of $C_{22}H_{22}O_{12}$ **(Fig. 5**).

3.6. Molecular docking

To shed light on DGL-M5ME binding interactions, *in silico* molecular docking was performed using AutoDock Vina program. The open conformation of DGL, in complex with a phosphonate inhibitor covalently bound to its catalytic serine residue [24], was used as reference model to improve the reliability of docking results. The lipase active site was found to be fully accessible thus enabling docking experiments. Automated docking resulted in several possible conformations of the M5ME inhibitor within DGL catalytic pocket, with favorable binding energies ranging from -8.3 to -9.5 kcal/mol **(Fig. S3A**). For subsequent analysis, we retained the best matching conformation that directly exposes the most reactive carbon atom of the M5ME inhibitor towards the catalytic serine, within a calculated distance of 3.8 Å which is sufficient to promote the nucleophilic attack **(Fig. S3B)**. In this configuration, we found that M5ME could fit properly into DGL catalytic pocket **(Fig. 6)**, which consists of a deep canyon of approximately 20 Å long, 7 Å wide, and 20 Å deep [24]. Moreover, like the phosphonate inhibitor, M5ME shows a relatively flat structure, with measured lengths of around 12 Å long, 5.5 Å wide, and 9 Å deep **(Fig. S3C)**. For the sake of comparison, the previously reported phosphonate inhibitor only measures 6 Å long, 2 Å wide and 10 Å deep, and thus requires the presence of β-octyl glucoside or 1-amino-anthracene to completely fill the catalytic pocket [24]. Interestingly, a more detailed analysis of the environment of the M5ME compound, bond to the catalytic serine, revealed a significant stabilizing effect of the DGL-M5ME tetrahedral

316 intermediate by the neighboring oxyanion hole **(Fig. 5)**. Indeed, an oxygen originating from
317 the pyran ring of M5ME points towards the backbone nitrogen atoms of Leu67 and Gln154
318 residues within hydrogen bond distances of 2.37 Å and 2.08 Å, respectively.

319 **4. Discussion**

320 Star anise (*Illicium verum*) is an important traditional Chinese medicine as well as a
321 commonly used spice. Its tree is an aromatic evergreen tree growing almost exclusively in
322 southern China and Vietnam. The fruit of star anise is used in traditional medicine to treat
323 stomachache, colic, vomiting, insomnia, skin inflammation, rheumatic pain, dyspepsia, facial
324 paralysis, asthma, and bronchitis [33]. A great deal of research effort is being devoted to testing
325 the putative beneficial effects of star anise extracts. Modern pharmacology studies
326 demonstrated that crude extracts and active compounds of star anise possess wide
327 pharmacological actions [34]. However, to the best of our knowledge, none has yet examined
328 the effect of star anise extracts on digestive lipases activities.

329 DGL provides a good model for human gastric lipases [24, 35]. A screening of a collection
330 of 20 extracts from five medicinal plants using solvents with different polarities allowed the
331 identification of ethanolic extract from star anise, which efficiently inhibited gastric lipase
332 **(Table S1)**. The inhibitory effect of star anise ethanolic extract on DGL might be caused by
333 the presence of phenolic compounds within the extract. It was reported that ethanol/water
334 extracts of star anise contained high amounts of phenolic compounds [36]. The use of water in
335 combination with ethanol contributes to the creation of a moderately polar medium that
336 ensures the extraction of phenolic compounds [37]. Plant phenolic compounds, such as flavones,
337 flavanols, tannins and chalcones, have been reported as pancreatic lipase inhibitors [14], thus
338 supporting the use of star anise polyphenolic-rich extract for further bioactivity guided
339 fractionation **(Fig. 1)**.

Our results showed that removal of lipoidal material from star anise before phenolic extraction enhanced anti-lipase activity, which might be related to the fact that the concentration of phenolics in SACPE is lower than in SAPE, suggesting thereby that the anti-lipase effect is related to star anise phenolic compounds. One of the hallmarks of bioactivity guided fractionation is the trend of increasing potency with increasing fractionation. Indeed, the a_I value that totally abolishes gastric lipase activity moved from 1 mg SAPE to 30 µg SAPRF4 after two fractionation steps. According to TLC analysis, SAPRF4 produced by this fractionation approach is a less complex mixture than the initial SAPE **(Fig. S1)**. We therefore sought to evaluate SAPRF4 potency and selectivity against other lipases of medicinal interest.

Inhibiting lipases has potential applications in the field of medicine. The digestive lipase inhibitor Orlistat used for the treatment of obesity has been shown to also inhibit HSL [38] and microbial lipases [8, 39]. In the sake of comparison, SAPRF4 was found to inhibit efficiently DGL, HPL, and LipY (a microbial lipase belonging to the HSL family). The ability of SAPRF4 to inhibit the catalytic activity of these lipases was assessed in terms of a_{I50} and $t_{½}$ values **(Table 1)**. The inhibition of HSL could be a potential approach to reduce levels of circulating FFAs linked to insulin resistance in obese patients [40]. Consequently, SAPRF4 might be an effective candidate for the treatment of obesity and diabetes. Moreover, as LipY contributes to the growth and pathogenicity of *M. tuberculosis* [26], it would be a therapeutic target for SAPRF4 as an anti-microbial agent.

On the bioaffinity interaction level, inhibitors can bind either covalently or non-covalently with their biological target [41]. In the cases of non-covalent inhibition, the inhibitor does not bind covalently with the biological target. Thereby, non-covalent inhibitor compounds are of no special interest in drug discovery projects [16]. MALDI-TOF mass spectrometry is an analytical instrument tool that can measure protein-inhibitor complex mass when a specific covalent binding occurs, reflecting thereby an approximate molecular mass of

365 the inhibitor [38]. Direct MALDI-TOF mass spectrometry analysis of DGL totally inhibited by
366 SAPRF4 showed the occurrence of an increase in the molecular masses of DGL, which is
367 compatible with the formation of a covalent complex with the inhibitor. PMF analysis of a
368 trypsin digest of DGL inhibited or not with SAPRF4 showed an increase in the molecular
369 mass of the catalytic serine-containing peptide **(Fig. 4)** corresponding in size to the
370 approximate molecular mass of the inhibitor. This process might involve a nucleophilic attack
371 between the enzyme's catalytic serine and the inhibitor, leading to the formation of a covalent
372 inhibitor-modified enzyme. Based on PMF analysis, it has been also shown previously that
373 synthetic inhibitors, oxadiazolones [28] and cyclophostin analogs [8, 42], form a covalent bond
374 with the catalytic serine residue of lipases. To the best of our knowledge, this is the first study
375 that used covalent inhibitor-modified enzyme complex data to tentatively identify a lipase
376 inhibitor in a natural extract.

377 Achieving the approximate molecular mass of the covalent lipase inhibitor, the
378 identification of the compound of interest within SAPRF4 would be rather more
379 straightforward. Thus, using the inhibitor mass information, we applied UPLC-HRMS for
380 mass-directed screening to tentatively identify the expected lipase inhibitor in SAPRF4. Using
381 this non-target screening, it was possible to separate and detect seven chromatographic peaks
382 containing high resolution MS information **(Fig. S2)**. The tentative identification of these
383 peaks was performed according to their high-resolution accurate mass and isotopic patterns to
384 empirically determine their molecular formulas. By inspecting all mass spectra around m/z of
385 489.52 in the chromatogram of SAPRF4, one ion having m/z of 479.1187 was found to fit
386 with PMF analysis data. This ion, assigned to the molecular formula $C_{22}H_{22}O_{12}$, corresponds
387 likely to the flavonoid myricitrin-5-methyl ether **(Fig. 5)** that has not been identified
388 previously from star anise.

To gain insights into the lipase-inhibitor binding interactions at the molecular level, M5ME was docked into the active site of DGL **(Fig. 6)**. The final selection of M5ME "bioactive" conformation suggests that the inhibition mechanism involve a nucleophilic attack by the hydroxy group of the catalytic Ser on a reactive carbon atom of the inhibitor pyran ring, thus leading to the formation of a stoichiometric enzyme-inhibitor covalent complex **(Fig. 5)**. Interestingly, the nucleophilic attack could be favored by some surrounding residues, including the backbone nitrogen atoms of Leu^{67} and Gln^{154} that belong to the previously described DGL oxyanion hole [24].

Much more interest has been shifted on plant flavonoids for their possible anti-obesity effects. *In vitro* and *in vivo* studies provided evidence on the potential role that flavonoids play in the management of obesity [43]. M5ME, a myricetin glycoside, was isolated from the flower of *Rhododendron poukhanense* as a potent antioxidant flavonoid. Although no lipase inhibiting activity was reported in the literature for M5ME, the structurally fairly similar quercetin and kaemferol were reported to be potent pancreatic lipase inhibitors [44]. Moreover, myricetin was found to exert *in vivo* a strong anti-obesity and anti-hyperlipidaemic activities by modulating the lipid metabolism [45].

To our knowledge, this is the first report that tentatively identified a new natural gastric lipase inhibitor from a natural product. The combination of *in silico* molecular docking results with those of lipase inhibition and mass spectrometry provides a scientific evidence for the potential medicinal use of the flavonoid myricitrin-5-methyl ether as a lipase inhibitor for the treatment of obesity, type 2 diabetes and tuberculosis.

Author contributions

J.K. carried out experiments and performed analyses. R.R., M.S., P.M., R.L. and A.B.-B. contributed to experiments realization and analysis. I.K., K.A., A.A. and F.C. contributed to experiments design and analysis. J.K. and A.A. conceived experiments and wrote the paper.

Declaration of interests

There are no conflicts of interest to declare.

Acknowledgments

This work was supported by the Ministry of Higher Education and Scientific Research, Tunisia. Dr. Stéphane Canaan and Dr. Jean-François Cavalier (CNRS, Marseille) are acknowledged for their generous gift of LipY enzyme and for useful discussions.

References

1. A. Aloulou and F. Carriere, Gastric lipase: an extremophilic interfacial enzyme with medical applications, *Cell Mol Life Sci*, 2008, **65**, 851-854.
2. A. Aloulou, D. Puccinelli, J. Sarles, R. Laugier, Y. Leblond and F. Carriere, In vitro comparative study of three pancreatic enzyme preparations: dissolution profiles, active enzyme release and acid stability, *Aliment Pharmacol Ther*, 2008, **27**, 283-292.
3. F. Carriere, E. Rogalska, C. Cudrey, F. Ferrato, R. Laugier and R. Verger, In vivo and in vitro studies on the stereoselective hydrolysis of tri- and diglycerides by gastric and pancreatic lipases, *Bioorganic & medicinal chemistry*, 1997, **5**, 429-435.
4. F. Carriere, J. A. Barrowman, R. Verger and R. Laugier, Secretion and contribution to lipolysis of gastric and pancreatic lipases during a test meal in humans, *Gastroenterology*, 1993, **105**, 876-888.

5. H. Lengsfeld, Physiology of Gastrointestinal Lipolysis and Therapeutical Use of Lipases and Digestive Lipase Inhibitors, *Lipases and Phospholipases in Drug Development: From Biochemistry to Molecular Pharmacology*, 2005, DOI: 10.1002/3527601910.ch10, 195-223.

6. H. L. Daneschvar, M. D. Aronson and G. W. Smetana, FDA-Approved Anti-Obesity Drugs in the United States, *Am J Med*, 2016, **129**, 879 e871-876.

7. F. Carriere, C. Renou, S. Ransac, V. Lopez, J. De Caro, F. Ferrato, A. De Caro, A. Fleury, P. Sanwald-Ducray, H. Lengsfeld, C. Beglinger, P. Hadvary, R. Verger and R. Laugier, Inhibition of gastrointestinal lipolysis by Orlistat during digestion of test meals in healthy volunteers, *American journal of physiology. Gastrointestinal and liver physiology*, 2001, **281**, G16-28.

8. V. Point, R. K. Malla, S. Diomande, B. P. Martin, V. Delorme, F. Carriere, S. Canaan, N. P. Rath, C. D. Spilling and J. F. Cavalier, Synthesis and kinetic evaluation of cyclophostin and cyclipostins phosphonate analogs as selective and potent inhibitors of microbial lipases, *J Med Chem*, 2012, **55**, 10204-10219.

9. L. Titta, M. Trinei, M. Stendardo, I. Berniakovich, K. Petroni, C. Tonelli, P. Riso, M. Porrini, S. Minucci, P. G. Pelicci, P. Rapisarda, G. Reforgiato Recupero and M. Giorgio, Blood orange juice inhibits fat accumulation in mice, *International journal of obesity*, 2010, **34**, 578-588.

10. R. B. Birari, S. Gupta, C. G. Mohan and K. K. Bhutani, Antiobesity and lipid lowering effects of Glycyrrhiza chalcones: experimental and computational studies, *Phytomedicine : international journal of phytotherapy and phytopharmacology*, 2011, **18**, 795-801.

11. Y. Gu, W. J. Hurst, D. A. Stuart and J. D. Lambert, Inhibition of key digestive enzymes by cocoa extracts and procyanidins, *Journal of agricultural and food chemistry*, 2011, **59**, 5305-5311.

12. M. Yoshikawa, H. Shimoda, N. Nishida, M. Takada and H. Matsuda, Salacia reticulata and its polyphenolic constituents with lipase inhibitory and lipolytic activities have mild antiobesity effects in rats, *The Journal of nutrition*, 2002, **132**, 1819-1824.

13. N. Yuda, M. Tanaka, M. Suzuki, Y. Asano, H. Ochi and K. Iwatsuki, Polyphenols extracted from black tea (Camellia sinensis) residue by hot-compressed water and their inhibitory effect on pancreatic lipase in vitro, *Journal of food science*, 2012, **77**, H254-261.

14. R. B. Birari and K. K. Bhutani, Pancreatic lipase inhibitors from natural sources: unexplored potential, *Drug discovery today*, 2007, **12**, 879-889.

15. F. E. Koehn and G. T. Carter, The evolving role of natural products in drug discovery, *Nat Rev Drug Discov*, 2005, **4**, 206-220.

16. M. G. Weller, A unifying review of bioassay-guided fractionation, effect-directed analysis and related techniques, *Sensors (Basel)*, 2012, **12**, 9181-9209.

17. S. A. Hofstadler and K. A. Sannes-Lowery, Applications of ESI-MS in drug discovery: interrogation of noncovalent complexes, *Nat Rev Drug Discov*, 2006, **5**, 585-595.

18. L. L. Cummins, S. Chen, L. B. Blyn, K. A. Sannes-Lowery, J. J. Drader, R. H. Griffey and S. A. Hofstadler, Multitarget affinity/specificity screening of natural products: finding and characterizing high-affinity ligands from complex mixtures by using high-performance mass spectrometry, *J Nat Prod*, 2003, **66**, 1186-1190.

19. B. M. Johnson, D. Nikolic and R. B. van Breemen, Applications of pulsed ultrafiltration-mass spectrometry, *Mass Spectrom Rev*, 2002, **21**, 76-86.

481 20. H. Vu, N. B. Pham and R. J. Quinn, Direct screening of natural product extracts using
482 mass spectrometry, *J Biomol Screen*, 2008, **13**, 265-275.
483 21. D. C. Hilton, R. S. Jones and A. Sjodin, A method for rapid, non-targeted screening
484 for environmental contaminants in household dust, *J Chromatogr A*, 2010, **1217**,
485 6851-6856.
486 22. M. Ibáñez, J. V. Sancho, F. Hernández, D. McMillan and R. Rao, Rapid non-target
487 screening of organic pollutants in water by ultraperformance liquid chromatography
488 coupled to time-of-light mass spectrometry, *TrAC Trends in Analytical Chemistry*,
489 2008, **27**, 481-489.
490 23. M. A. Ramirez-Coronel, N. Marnet, V. S. Kolli, S. Roussos, S. Guyot and C. Augur,
491 Characterization and estimation of proanthocyanidins and other phenolics in coffee
492 pulp (Coffea arabica) by thiolysis-high-performance liquid chromatography, *Journal*
493 *of agricultural and food chemistry*, 2004, **52**, 1344-1349.
494 24. A. Roussel, N. Miled, L. Berti-Dupuis, M. Riviere, S. Spinelli, P. Berna, V. Gruber, R.
495 Verger and C. Cambillau, Crystal structure of the open form of dog gastric lipase in
496 complex with a phosphonate inhibitor, *J Biol Chem*, 2002, **277**, 2266-2274.
497 25. V. Belle, A. Fournel, M. Woudstra, S. Ranaldi, F. Prieri, V. Thome, J. Currault, R.
498 Verger, B. Guigliarelli and F. Carriere, Probing the opening of the pancreatic lipase lid
499 using site-directed spin labeling and EPR spectroscopy, *Biochemistry*, 2007, **46**, 2205-
500 2214.
501 26. P. Santucci, S. Diomande, I. Poncin, L. Alibaud, A. Viljoen, L. Kremer, C. de
502 Chastellier and S. Canaan, Delineating the physiological roles of the PE and catalytic
503 domain of LipY in lipid consumption in mycobacteria-infected foamy macrophages,
504 *Infect Immun*, 2018, DOI: 10.1128/IAI.00394-18.

27. C. Chapus, P. Desnuelle and E. Foglizzo, Stabilization of the C-terminal part of pig and horse colipase by carboxypeptidase and trypsin inhibitors, *Eur J Biochem*, 1981, **115**, 99-105.

28. V. Point, K. V. Pavan Kumar, S. Marc, V. Delorme, G. Parsiegla, S. Amara, F. Carriere, G. Buono, F. Fotiadu, S. Canaan, J. Leclaire and J. F. Cavalier, Analysis of the discriminative inhibition of mammalian digestive lipases by 3-phenyl substituted 1,3,4-oxadiazol-2(3H)-ones, *Eur J Med Chem*, 2012, **58**, 452-463.

29. O. Trott and A. J. Olson, AutoDock Vina: improving the speed and accuracy of docking with a new scoring function, efficient optimization, and multithreading, *J Comput Chem*, 2010, **31**, 455-461.

30. E. F. Pettersen, T. D. Goddard, C. C. Huang, G. S. Couch, D. M. Greenblatt, E. C. Meng and T. E. Ferrin, UCSF Chimera--a visualization system for exploratory research and analysis, *J Comput Chem*, 2004, **25**, 1605-1612.

31. M. D. Hanwell, D. E. Curtis, D. C. Lonie, T. Vandermeersch, E. Zurek and G. R. Hutchison, Avogadro: an advanced semantic chemical editor, visualization, and analysis platform, *J Cheminform*, 2012, **4**, 17.

32. J.-C. Charrié, B. Chastel, C. Cieur, P. Combe, M. Damak, K. Hedayat and C. Saigne-Soulard, *Plantes médicinales - Phytothérapie clinique intégrative et médecine endobiogénique*, Lavoisier S.A.S., 2017.

33. Y. Y. Sung, W. K. Yang, A. Y. Lee, D. S. Kim, K. J. Nho, Y. S. Kim and H. K. Kim, Topical application of an ethanol extract prepared from Illicium verum suppresses atopic dermatitis in NC/Nga mice, *J Ethnopharmacol*, 2012, **144**, 151-159.

34. G. W. Wang, W. T. Hu, B. K. Huang and L. P. Qin, Illicium verum: a review on its botany, traditional use, chemistry and pharmacology, *J Ethnopharmacol*, 2011, **136**, 10-20.

35. S. Fernandez, S. Chevrier, N. Ritter, B. Mahler, F. Demarne, F. Carriere and V. Jannin, In vitro gastrointestinal lipolysis of four formulations of piroxicam and cinnarizine with the self emulsifying excipients Labrasol and Gelucire 44/14, *Pharm Res*, 2009, **26**, 1901-1910.

36. A. Padmashree, N. Roopa, A. D. Semwal, G. K. Sharma, G. Agathian and A. S. Bawa, Star-anise (Illicium verum) and black caraway (Carum nigrum) as natural antioxidants, *Food Chemistry*, 2007, **104**, 59-66.

37. C. Liyana-Pathirana and F. Shahidi, Optimization of extraction of phenolic compounds from wheat using response surface methodology, *Food Chemistry*, 2005, **93**, 47-56.

38. Y. Ben Ali, H. Chahinian, S. Petry, G. Muller, R. Lebrun, R. Verger, F. Carriere, L. Mandrich, M. Rossi, G. Manco, L. Sarda and A. Abousalham, Use of an inhibitor to identify members of the hormone-sensitive lipase family, *Biochemistry*, 2006, **45**, 14183-14191.

39. R. Dhouib, A. Ducret, P. Hubert, F. Carriere, S. Dukan and S. Canaan, Watching intracellular lipolysis in mycobacteria using time lapse fluorescence microscopy, *Biochim Biophys Acta*, 2011, **1811**, 234-241.

40. G. Boden, Interaction between free fatty acids and glucose metabolism, *Curr Opin Clin Nutr Metab Care*, 2002, **5**, 545-549.

41. H. Gohlke and G. Klebe, Approaches to the description and prediction of the binding affinity of small-molecule ligands to macromolecular receptors, *Angew Chem Int Ed Engl*, 2002, **41**, 2644-2676.

42. V. Point, R. K. Malla, F. Carriere, S. Canaan, C. D. Spilling and J. F. Cavalier, Enantioselective inhibition of microbial lipolytic enzymes by nonracemic monocyclic enolphosphonate analogues of cyclophostin, *J Med Chem*, 2013, **56**, 4393-4401.

555 43. N. Al Shukor, K. Raes, G. Smagghe and J. Van Camp, in *Flavonoids and*
556 *antioxidants*, Studium Press LLC, New Delhi, India, 2016, vol. 40, pp. 496-514.
557 44. T. Sergent, J. Vanderstraeten, J. Winand, P. Beguin and Y.-J. Schneider, Phenolic
558 compounds and plant extracts as potential natural anti-obesity substances, *Food*
559 *Chemistry*, 2012, **135**, 68-73.
560 45. C. J. Chang, T. F. Tzeng, S. S. Liou, Y. S. Chang and I. M. Liu, Myricetin Increases
561 Hepatic Peroxisome Proliferator-Activated Receptor alpha Protein Expression and
562 Decreases Plasma Lipids and Adiposity in Rats, *Evid Based Complement Alternat*
563 *Med*, 2012, **2012**, 787152.

564

565 **FIGURE LEGENDS**

566 **Fig. 1. Bioactivity-guided fractionation scheme of star anise.**

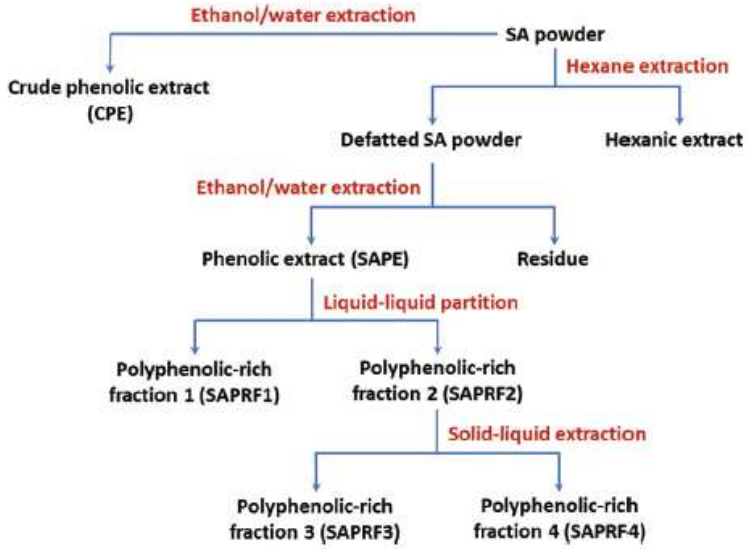

567

Fig. 2. Evaluation of the inhibitory effect of the SAPRF4 fraction against DGL, HPL and LipY lipases. Each lipase was pre-incubated in the presence of various SAPRF4 amounts for 30 min at 25 °C and residual activities of DGL (A), HPL (B) and LipY (C) were measured. Alternatively, residual activities of DGL (D), HPL (E) and LipY (F) were measured as a function of the incubation time at a constant SAPRF4 amount. The a_I value used in these latter experiments was chosen so that the average residual activities of DGL, HPL and LipY obtained after 30 min of incubation were in the 15-20 % range. Results are expressed as mean values of at least three independent assays.

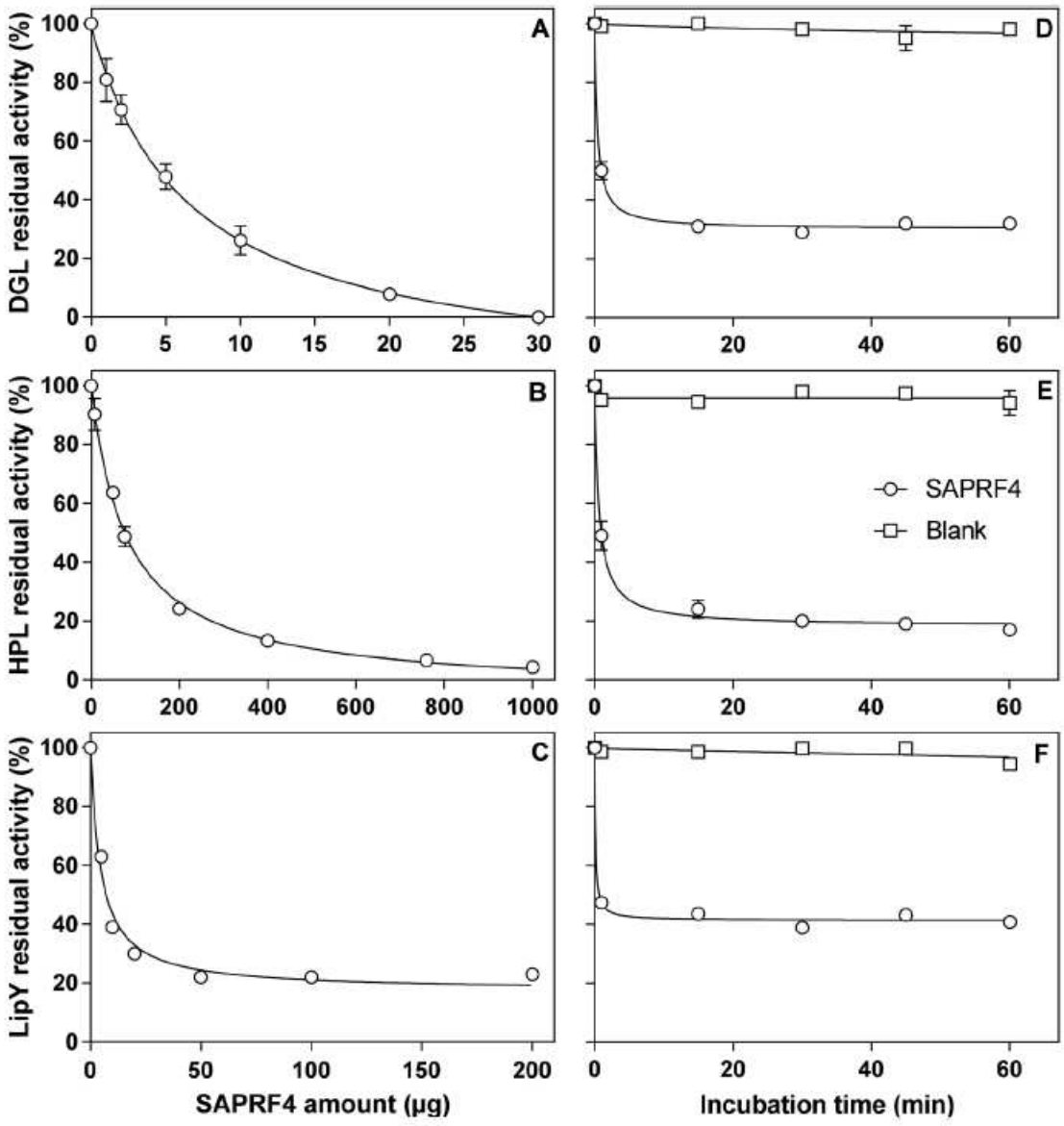

577 **Fig. 3. MALDI-TOF mass spectrometry analysis of untreated (grey spectrum) and**
578 **treated (black spectrum) DGL.** A 30-min incubation was performed at 25 °C in the
579 presence or absence of SAPRF4 amount of 30 µg.

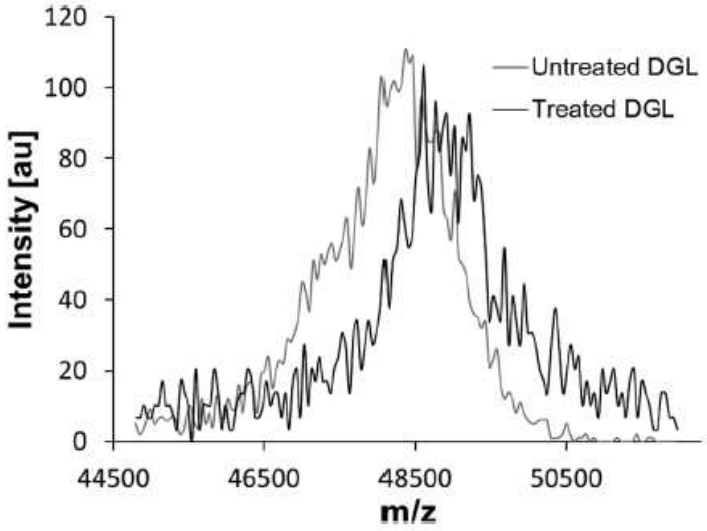

580

Fig. 4. PMF spectra of untreated (A) and treated (B) DGL. A 30-min incubation was performed at 25 °C in the presence or absence of SAPRF4 amount of 30 µg. Left panels, region of the unmodified isotopic peptide L^{147}-K^{168} containing the catalytic Ser^{153} and detected at 2376.05 Da. This peak is overlaid with a second one corresponding to the peptide detected at 2414.82 Da. Right panels, region in which a new isotopic peptide was expected to occur, resulting from the covalent binding of the natural inhibitor of interest to the catalytic serine. Mass shift was calculated as the difference between the experimental m/z of the unmodified peptide and the theorical m/z of the unmodified peptide.

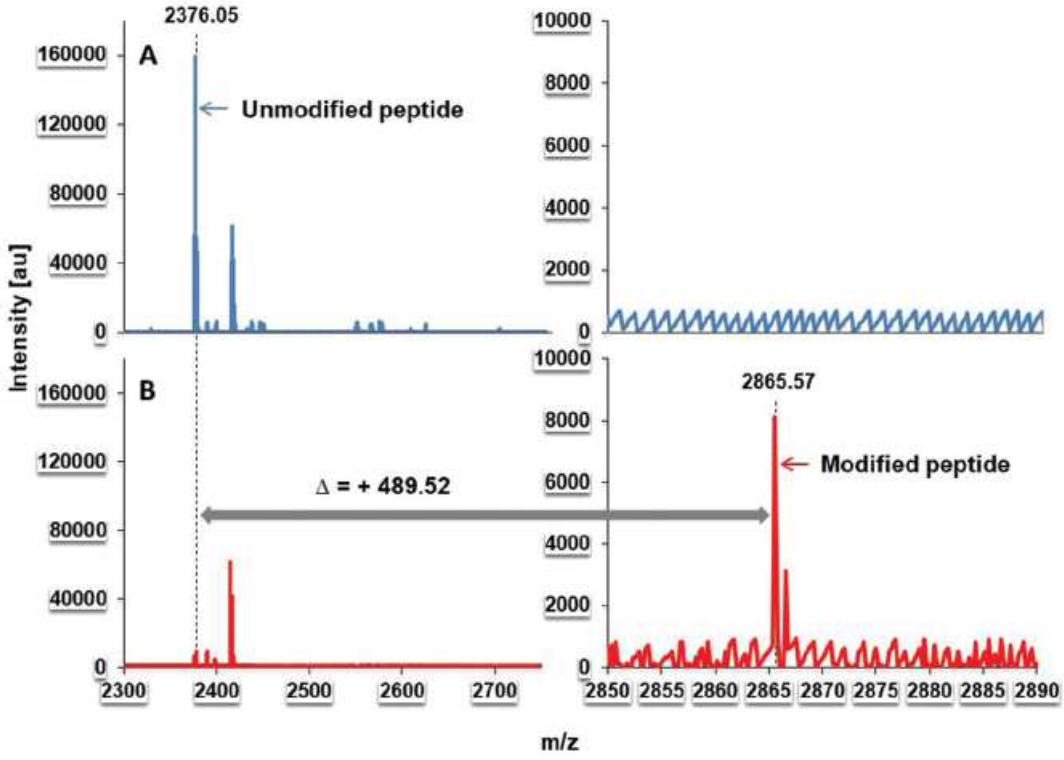

590 **Fig. 5. Chemical structure of the flavonoid myricitrin-5-methyl ether (M5ME) and**
591 **proposed mechanism underlying DGL inhibition by M5ME.** The nucleophilic attack by
592 the hydroxyl group of the catalytic Ser^{153} residue on the inhibitor reactive site leads to a 1,4-
593 nucleophilic addition on a double bond conjugated to a ketone and the formation of an enol
594 function.

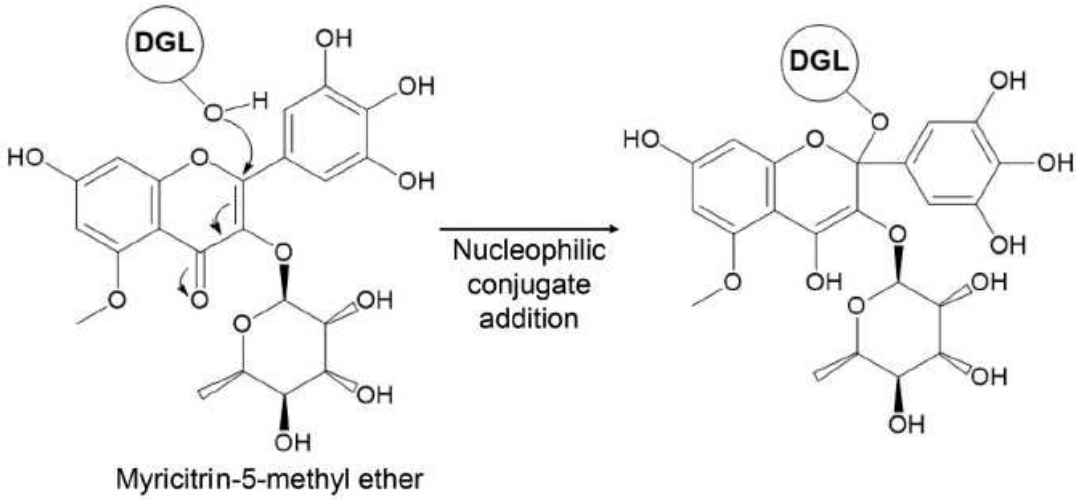

595

596 **Fig. 6. Visualization of DGL-M5ME binding interaction by molecular docking.** A,
597 molecular surface representation of DGL active site crevice with the bound M5ME. B, view
598 of the active site of DGL with the bound M5ME. The backbone nitrogens of residues Leu^{67}
599 and Gln^{154} are at hydrogen bonding distance from an oxygen atom originating from the
600 inhibitor. The catalytic residues Ser^{153}, His^{353} and Asp^{324} are highlighted in pink and the
601 inhibitor is represented in CPK coloring (oxygen, red).

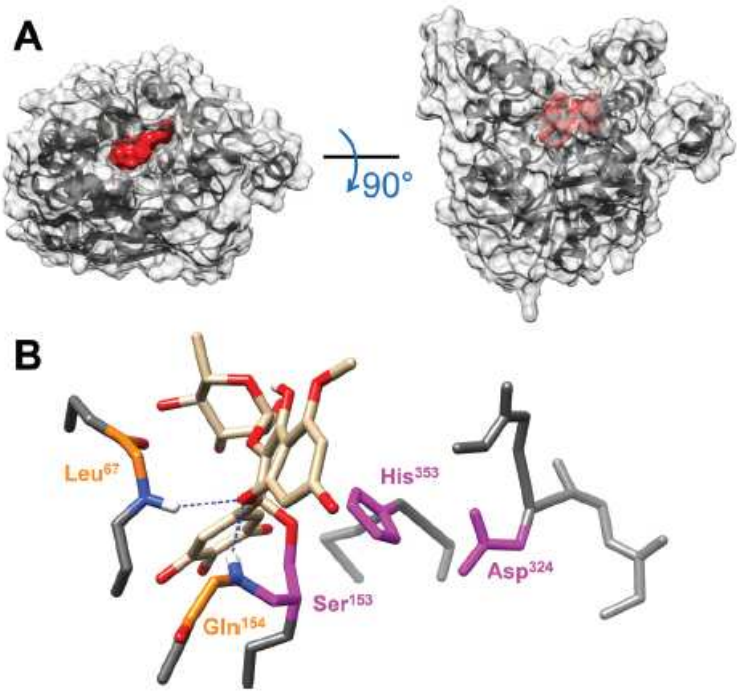

602

603

Table 1. a_{I50} and $t_{½}$ values of SAPRF4 on DGL, HPL and LipY.*

Lipases	a_{I50} (µg)	$t_{½}$ (min)
DGL	7	0.4
HPL	82	0.6
LipY	5	0.1

* SAPRF4 amount (a_I) used for the determination of $t_{½}$ was 10 µg, 200 µg and 10 µg for DGL, HPL and LipY, respectively. Results are expressed as mean values of at least three independent assays (CV % < 5.0%).